MHD Nanofluid Flow with Gyrotactic Microorganisms on a Sheet Embedded in a Porous Medium

Batool, Maria; Ashraf, Muhammad*[+]

Centre for Advanced Studies in Pure and Applied Mathematics (CASPAM),
Bahauddin Zakariya University, Multan, PAKISTAN

ABSTRACT: *A numerical study of MHD nanofluid flow with gyrotactic microorganisms due to a stretching sheet embedded in a porous media is presented. The governing nonlinear Partial Differential Equations (PDEs) are transformed into corresponding ordinary ones through a power tool of similarity transformation. Impressions of important parameters on physical measures through tables as well as figures are discussed. The applied magnetic field tends to rise the shear stress while reducing the rates of heat transfer, nanoparticle volume fraction, and density of microorganisms. The porous medium causes a reduction in velocity distribution while it grows other measures like temperature, nanoparticle volume fraction, and microorganism's density. The present work has various applications in industry, technology, and biosciences.*

KEYWORDS: *Heat Transfer; Magnetic Field; Stretching Velocity; Quasi-Linearization; Nanoparticle; Volume Fraction.*

INTRODUCTION

Nanofluid is a type of medium that holds tiny and microparticles are known as nanoparticles or microbes. These tiny particles can contribute to enhancing thermal conductivity when added to the base fluid. These particles support improving heat transfer characteristics of nanofluid. There are voids in a porous medium. Naturally, there are numerous porous mediums accessible. Limestones, beach sand, rye dough, dolomite & pumice, lung of human and injecting drugs through human skin are a few examples of porous media. Flows passing through the porous region have fascinated the researchers as well as have provided a diverse field of research. MHD nanofluid flows with gyrotactic microorganisms have well-known and mesmerizing contributions in the fields of biomedical and industry. The swimming of moving microorganisms creates a wonder is known as bioconvection. The motile microorganisms are self-driven but the nanoparticles move under influence of thermophoresis impact & Brownian motion. In the reduction of greenhouse impact, microorganisms have a positive role. In comparison with trees, some microorganisms such as germs, dictums, and foam absorbs more CO_2. Previously, impacts of viscous dissipation and heat transfer in nano liquid were investigated by researchers. Further, the study of nanofluid-containing microorganisms under influence of mixed convection was also conducted in porous media. In our present work, we have considered the flow problem of MHD nanofluid having microorganisms through the porous medium. This current study has various advantages in mechanical engineering, biomedical science, and technology. For example, this present investigation is advantageous in materials of building insulation, permeation of medicine

***** *To whom correspondence should be addressed.*
+ *E-mail*: *mashraf_mul@yahoo.com*
1021-9986/2021/5/1693-1702 *10/$/6.00*

through human skin, solar heating, and cooling systems, ventilation, devices of heat exchange, etc.

Mahat et al. [1] numerically studied boundary layer mixed convection flow of viscoelastic nanofluid through circular cylinder while considering convective boundary condition. Mass, as well as heat transfer features in MHD squeezing flow of nanofluid between two plates, were examined numerically by *Husseinzadhe et al.* [2]. *Muhammad et al.* [3] investigated the impact of thermal radiation on the MHD bioconvection flow of nanofluid on a parallel plate. *Aziz et al.* [4] scrutinized the heat transfer characteristics in flow of nanofluid past an unsteady stretching sheet. *Iqbal et al.* [5] have investigated heat and mass transfer in an unsteady incompressible viscous hydromagnetic nanofluid between two orthogonally moving coaxial porous disks under the influence of suction parameter. The impact of EMHD in nanofluid flow over a Riga porous plate is numerically investigated by *Abbas et al.* [6] in the presence of Lorentz force that acts parallel to the wall of the Riga surface. *Sibanda* and *Khidir* [7] inspected the flow of electrically conducting nanofluid past a nonlinearly stretching sheet with viscous dissipation as well as discussed influences of thermophoresis, Brownian motion and nanoparticle volume fraction on convective heat transfer. The stimulus of combined double-diffusive and viscous dissipation due to a vertical semi-infinite plate embedded in a porous non-Darcy medium by using non-uniform boundary conditions was numerically evaluated by *Aghbari et al.* [8]. *Kumar* and *Mishra* [9] examined the effect of thermal radiation, viscous dissipation, injection/suction, and Joule heating on MHD flow of nanofluids on a stretching flat sheet in a porous medium with water as a base fluid. *Yusuri et al.* [10] numerically analyzed the natural convection flow of nano liquid in a square. They found the solution of discretized equations by using SIMPLE procedure. *Ashraf et al.* [11] employed the Runge-Kutta scheme to compute the numerical solution of the problem of micropolar fluid flow in a porous Darcy-Forchheimer channel. *Kumara et al.* [12] scrutinized nonlinear radiation's influence on heat transfer as well as boundary layer Casson nanofluid flow due to nonlinearly elongating sheet involving chemical reaction and gained outcomes numerically by employing representative software of MAPLE. *Kumar* and *Pandey* [13] numerically observed the impact of mass transfer and heat on the flow of nanofluid flow over an enlarging sheet with the contribution of viscous dissipation, radiation, and generation /absorption of heat. The upshot of bioconvection in magneto-nano liquid due to a stretched-out sheet with gyrotactic microorganisms under velocity slip of second-order was surveyed by *Sampath et al.* [14]. *Sheikholeslami et al.* [15] inspected the hydrothermal conduct of refrigerant-based nanofluid with *CuO* and *R600a* chosen as nanoparticle and base fluid during compression inside a horizontal tube as well as the quality of vapor, mass flux, and concentration of nanoparticles. The investigation to estimate the enrichment of nanofluid heat transfer in a twisted pipe with the involvement of an alternate axis using twisted tape was performed by *Jafaryar et al.* [16]. *Rashad* and *Nabwey* [17] addressed the experimental analysis of bioconvection in a nanofluid with microorganisms through a circular horizontal cylinder and evaluated the impacts of thermophoresis, Brownian motion parameter as well as buoyancy ratio in fluid flow. *Ahmad et al.* [18] described the problem of micropolar fluid flow under influence of thermal radiation through porous media and found the numerical solution of resulting coupled ODEs by quasi-linearization.

This contemporary analysis of MHD nanofluid flow with gyrotactic microorganisms past a porous region has eminent practical applications in various fields. The purpose of this research is not only to observe the impact of numerous parameters on MHD nanofluid flow on a stretching sheet with gyrotactic microorganisms while the magnetic field is applied but also to provide an easy method to numerically solve a coupled system of nonlinear differential equations. Governing differential equations of our flow problem are altered into a system of self-similar equations by employing suitable transformations. Further, these self-similar forms are solved by the numerical method of quasi-linearization because it has fast convergence. Moreover, we have solved this flow problem in a single phase. The outcomes of our research are explained with the assistance of tables and figures of various physical measures employed in flow problems under consideration *via* the computing tool of MATLAB.

THEORETICAL SECTION

Mathematical derivation

Consider two-dimensional steady MHD nanofluid flow on a sheet with gyrotactic microorganisms in a porous medium. The flow has laminar conduct. The velocity has form $U_w = a_0x$ with x is the coordinate computed along stretching surface and a_0 is a constant. The magnetic field is applied to flow in a positive y-direction. The geometry of the current problem is given below in Fig. 1:

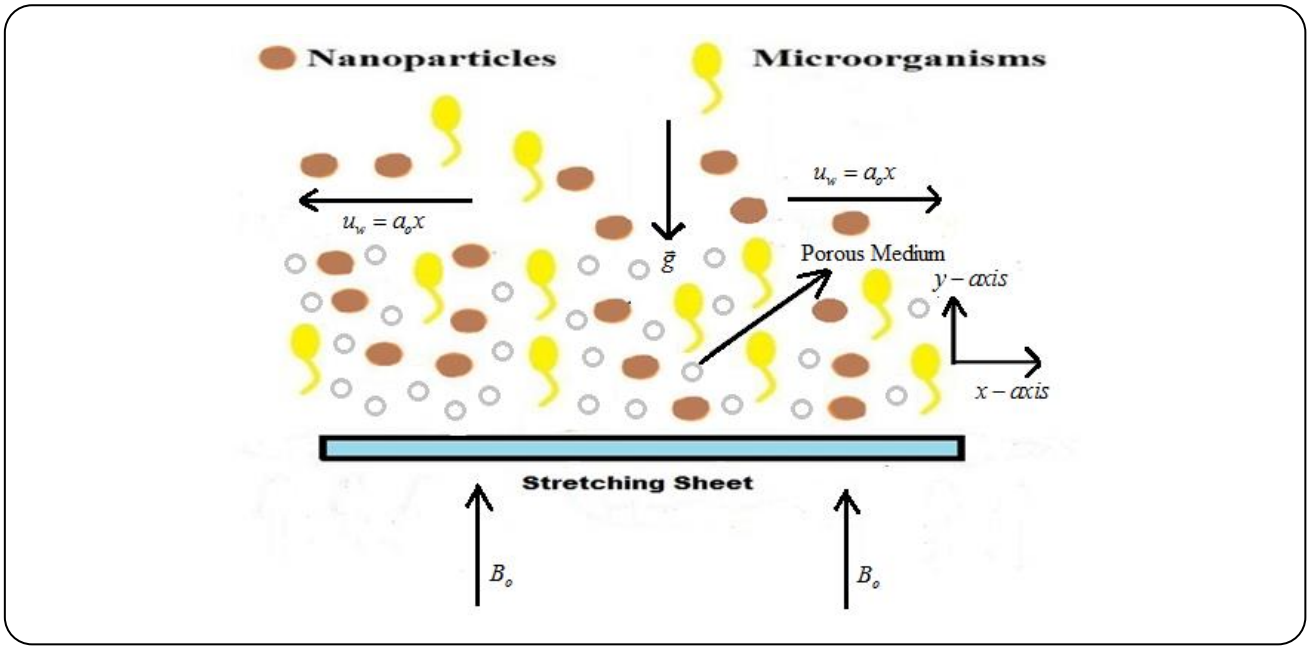

Fig. 1: The geometry of flow problem.

By following *Kausar et. al* [19], the governing Partial Differential Equations (PDEs) for problem of flow are:

$$\frac{\partial u}{\partial x}+\frac{\partial v}{\partial y}=0 \tag{1}$$

$$u\frac{\partial u}{\partial x}+v\frac{\partial u}{\partial y}=\upsilon\frac{\partial^2 u}{\partial y^2}-\frac{\sigma_c B_o^2}{\rho_{fl}}u-\frac{\upsilon}{k_o}u \tag{2}$$

$$u\frac{\partial T}{\partial x}+v\frac{\partial T}{\partial y}=\alpha\frac{\partial^2 T}{\partial y^2}+\tau\left\{D_b\frac{\partial c}{\partial y}\frac{\partial T}{\partial y}+D_t\left(\frac{\partial T}{\partial y}\right)^2\right\} \tag{3}$$

$$u\frac{\partial c}{\partial x}+v\frac{\partial c}{\partial y}=D_b\frac{\partial^2 c}{\partial y^2}+\frac{D_t}{T_f}\frac{\partial^2 T}{\partial y^2} \tag{4}$$

$$u\frac{\partial n}{\partial x}+v\frac{\partial n}{\partial y}+\frac{b_{ch}W_{cs}}{(c_w-c_f)}\left\{\frac{\partial}{\partial y}\left(n\frac{\partial c}{\partial y}\right)\right\}=D_m\frac{\partial^2 n}{\partial y^2} \tag{5}$$

Where u and v are velocity components, kinematic viscosity is υ, fluid temperature is T, σ_c is electric conductivity, α is the thermal diffusivity, B_o is the magnetic field strength, coefficient of thermophoresis diffusion is denoted by D_t, D_b is Brownian coefficient, D_m is the microorganism diffusion coefficient, chemotaxis constant is b_{ch}, W_{cs} is maximum swimming speed of cell ($b_{ch}W_{cs}$ is constant), ρ_{pr} is particle's density, ρ_{fl} is fluid's density, n denotes microorganisms' concentration, volume fraction of nanoparticles is denoted by c, $\tau=(\rho c)_{pr}/(\rho c)_{fl}$ is the ratio of effective heat capacity of the particle to the fluid. It is essential to point out that we have ignored the second-order inertial term in Eq. (2) because it involves a function that depends on Reynolds number which is small in the case of laminar fluid flow [20, 21].

The Boundary Conditions (BCs) associated with Eqs. (1)– (5) are given here:

$$v=0,\ u=\lambda U_w,\ T=T_w,\ c=c_w,\ n=n_w,\ for\ y=0 \tag{6}$$

$$u\to 0,\ T\to T_f,\ c\to c_f,\ n\to n_f,\ when\ y\to\infty \tag{7}$$

Where λ denotes a constant term, for stretching $\lambda>0$ and for shrinking $\lambda<0$. The subscript w shows the values at the boundary and the subscript f represents values far from the boundary. The governing (PDEs) are converted into a simpler form by employing variables of similarity which have the following mathematical form:

$$\eta=\left(\frac{a_0}{\upsilon}\right)^{1/2}y,\ \psi=(a_o\upsilon)^{1/2}x\,f(\eta), \tag{8}$$

$$\theta(\eta)=\frac{T-T_f}{T_w-T_f},\ \phi(\eta)=\frac{c-c_f}{c_w-c_f},$$

$$\chi(\eta)=\frac{n-n_f}{n_w-n_f}$$

The velocity components $u = \frac{\partial \psi}{\partial y}, v = -\frac{\partial \psi}{\partial x}$ assist to develop stream function ψ and η denotes the dimensionless similarity variable. The components *u* and *v* help to satisfy Eq. (1) in form of ψ. The transformation specified in (8) can be exploited to convert Eqs. (2) – (5) into ODEs given below:

$$f''' + ff'' - f'^2 - M(f') - \gamma(f') = 0, \tag{9}$$

$$\frac{1}{Pr}(\theta'') + f\theta' + \theta'\{N_b\phi' + N_t\theta'\} = 0 \tag{10}$$

$$\phi'' + \frac{N_t}{N_b}\theta'' + Le(f\phi') = 0, \tag{11}$$

$$\chi'' + Sc(f\chi') - Pe[\chi'\phi' + \phi''(\chi + \sigma)] = 0 \tag{12}$$

Also, BCs written in (6) as well as (7) have dimensionless form:

$$f = 0, f' = \lambda, \theta = 1, \phi = 1, \chi = 1, \quad at\ \eta = 0 \tag{13}$$

$$f' = 0, \ \theta = 0, \ \phi = 0, \ \chi = 0, \quad as\ \eta \to \infty \tag{14}$$

Where primes symbolize derivative w.r.t η. Further, *M* is a magnetic parameter, *Le* is Lewis number, N_t is thermophoresis parameter, *Pr* is Prandtl number, *Sc* is Schmidt number, N_b is Brownian motion parameter, *Pe* signifies Peclet number, σ is a constant term and γ is a porosity parameter, which has mathematical forms as:

$$N_t = \frac{\tau D_t (T_w - T_f)}{\upsilon}, \quad N_b = \frac{\tau D_b (c_w - c_f)}{\upsilon}, \quad Pr = \frac{\upsilon}{\alpha}, \tag{15}$$

$$Sc = \frac{\upsilon}{D_m}, Le = \frac{\upsilon}{D_b}, \quad M = \frac{\sigma_c B_o^2}{a_o \rho_{fl}}, \quad Pe = \frac{b_{ch} W_{cs}}{D_m},$$

$$\sigma = \frac{n_f}{(n_w - n_f)}, \ \gamma = \frac{\nu}{a_o k_o}$$

The nonlinear ODEs (9)-(12) accompanying with BCs specified in (13)-(14) are numerically explained by employing a procedure grounded on quasi-linearization.

In the process of quasi-linearization, we will develop sequences $(f^{(z)}), (f'^{(z)}), (\theta^{(z)}), (\phi^{(z)})$ and $(\chi^{(z)})$. Moreover, Eq. (9) is linearized to construct $(f^{(z)})$ by considering only the terms of the first order.

By operating on Eq. (9), we assume:

$$E(f, f', f'', f''') \equiv f''' + ff'' - f'^2 - Mf' - \gamma f', \tag{16}$$

$$E\left(f^{(z)}, f^{(z)\prime}, f^{(z)\prime\prime}, f^{(z)\prime\prime\prime}\right) + \left(f^{(z+1)} - f^{(z)}\right)\frac{\partial E}{\partial f^{(z)}} +$$

$$\left(f^{(z+1)\prime} - f^{(z)\prime}\right)\frac{\partial E}{\partial f^{(z)\prime}} + \left(f^{(z+1)\prime\prime} - f^{(z)\prime\prime}\right)\frac{\partial E}{\partial f^{(z)\prime\prime}} +$$

$$\left(f^{(z+1)\prime\prime\prime} - f^{(z)\prime\prime\prime}\right)\frac{\partial E}{\partial f^{(z)\prime\prime\prime}} = 0,$$

$$f^{(z+1)\prime\prime\prime} + f^{(z+1)\prime\prime}f^{(z)} - f^{(z+1)\prime}\left(M + \gamma + 2f^{(z)\prime}\right) +$$

$$f^{(z+1)}f^{(z)\prime\prime} = f^{(z)\prime\prime}f^{(z)}$$

In order to find the solution of ODEs, central difference approximations are operated to replace derivatives. Consequently, a linear system to produce sequence $(f^{(z)})$ is:

$$S\left(f^{(z+1)}\right) = T \ \text{ where } S = S\left(f^{(z)}\right) \text{ and } T = T\left(f^{(z)}\right)$$

By linearization of Eq. (10), we obtained:

$$\frac{1}{Pr}\theta^{(z+1)\prime\prime} + \theta^{(z+1)\prime}\left(f^{(z)} + 2N_b\phi^{(z)\prime} + 2N_t\right) + \tag{17}$$

$$N_b\theta^{(z)\prime}\phi^{(z+1)\prime} = N_b\theta^{(z)\prime}\phi^{(z)\prime}$$

Likewise, we can put Eq. (11) as well as Eq. (12) in form:

$$\phi^{(z+1)\prime\prime} + \frac{N_t}{N_b}\theta^{(z+1)\prime\prime} + Le f^{(z+1)}\phi^{(z+1)\prime} = 0 \tag{18}$$

$$\chi^{(z+1)\prime\prime} + Sc f^{(z+1)}\chi^{(z+1)\prime} - \tag{19}$$

$$Pe\left[\chi^{(z+1)\prime}\phi^{(z+1)\prime} + \phi^{(z+1)\prime\prime}\left(\chi^{(z+1)} + \sigma\right)\right] = 0$$

The steps which pay a role in computational technique to derive sequences $(f^{(z)}), (f'^{(z)}), (\theta^{(z)}), (\phi^{(z)})$ and $(\chi^{(z)})$ are:

I. Exploit given initial guesses $f^{(0)}, f'^{(0)}, \theta^{(0)}, \phi^{(0)}$ and $\chi^{(0)}$ which will satisfy the boundary conditions explained in Eqs. (13)- (14).

II. Utilize the given initial guesses in order to generate the new quantities $f^{(1)}, f'^{(1)}, \theta^{(1)}$ & $\phi^{(1)}$.

Table 1: Comparison between values of present & previous research due to numerous M.

M	$C_f Re_x^{1/2} = -f''(0)$		$Nu_x Re_x^{-1/2} = -\theta'(0)$	
	Aman et. al [22]	Present	Aman et al. [22]	Present
0	0	0	3.5583	3.5627
1	-2.8508	-2.8589	3.4822	3.4892
1.5	-4.5000	-4.5071	3.4589	3.4665
2	-6.2749	-6.2803	3.4415	3.4497

Table 2: Values of f''(0), θ'(0), ϕ'(0) & χ'(0) due to numerous M with N_b = 0.5, λ = 0.5, Pr = 4.6, Le = 2.7, Sc = 0.6, γ = 1.6, Pe = 0.2, N_t = 0.2, σ = 0.1.

M	f''(0)	θ'(0)	ϕ'(0)	χ'(0)
0	-0.7232	-0.2315	-0.5947	-0.3897
0.3	-0.7730	-0.2256	-0.5786	-0.3822
0.6	-0.8196	-0.2198	-0.5648	-0.3758
0.9	-0.8638	-0.2142	-0.5529	-0.3701
1.2	-0.9057	-0.2087	-0.5426	-0.3652
1.5	-0.9457	-0.2035	-0.5335	-0.3601

III. Engage the recently obtained quantities $f^{(1)}$ as well as $\phi^{(1)}$ to solve the linear system found from finite difference discretization of Eq. (19) to get value $\chi^{(1)}$.

IV. In the same way, use the values $f^{(1)}, f'^{(1)}, \theta^{(1)}, \phi^{(1)}$ and $\chi^{(1)}$ as initial guesses to repeat the procedure in order to find a new iteration. In conclusion sequences $\left(f^{(z)}\right), \left(f'^{(z)}\right), \left(\theta^{(z)}\right), \left(\phi^{(z)}\right)$ and $\left(\chi^{(z)}\right)$ are attained that converge to f, f', θ, ϕ and χ correspondingly.

V. The technique is continued to attain new iterations until

$$\max\left\{\left\|f^{(k+1)}-f^{(k)}\right\|_{L_\infty}, \left\|f'^{(k+1)}-f'^{(k)}\right\|_{L_\infty}, \left\|\theta^{(k+1)}-\theta^{(k)}\right\|_{L_\infty}, \left\|\phi^{(k+1)}-\phi^{(k)}\right\|_{L_\infty}, \left\|\chi^{(k+1)}-\chi^{(k)}\right\|_{L_\infty}\right\} < 10^{-7}$$

Validation of code

To evaluate the effectiveness of the code used in our problem, a table showing a comparison between the repercussions of present and previous literature is developed (see Table 1). The comparison is found to be in good agreement. So, it confirms the accuracy of our numerical solution technique.

RESULTS AND DISCUSSION

We portrayed velocity *f'(η)*, temperature *θ(η)*, motile microorganism's density *χ(η)* as well as the volume fraction of nanoparticles *ϕ(η)* and observed behaviors of their profiles under the impact of various parameters in the flow problem. We also inspected the influence of numerous parameters on the shear stress *f'(0)*, heat transfer rate *θ'(η)*, rate of nanoparticle volume fraction *ϕ'(0)* as well as density rate of microorganisms *χ'(0)* with the aid of tables. Table 1 describes a comparison between values of previous research outcomes of *f''(0)* and *θ'(0)* with current results. This association illustrates the convergence of numerical code.

It is noticed that when the magnetic field strength is higher than fluid density then shear stress on the sheet surface is enhanced and heat transfer rate decreases on the solid edge. One may notice that as compared to other measures, shear stress is significantly affected by magnetic parameter. Hence, Table 2 shows that as values of magnetic parameter *M* increase, *f''(0)* is growing while other three quantities *θ'(0)*, *ϕ'(0)* and *χ'(0)* are reducing.

Table 3: Values of f''(0), θ'(0), ϕ'(0) & χ'(0) due to numerous γ with N_b = 0.5, λ = 0.3, Pr = 4.4, Le = 2.7, Sc = 0.5, M = 0.7, Pe = 0.4, N_t = 0.2, σ = 0.1.

γ	f''(0)	θ'(0)	ϕ'(0)	χ'(0)
0.5	-0.3669	-0.1640	-0.4802	-0.4070
1	-0.4235	-0.1513	-0.4619	-0.3948
1.5	-0.4733	-0.1408	-0.4488	-0.3858
2	-0.5183	-0.1322	-0.4385	-0.3788
2.5	-0.5595	-0.1249	-0.4303	-0.3731
3	-0.5979	-0.1188	-0.4234	-0.3684

Table 4: Values of f''(0), θ'(0), ϕ'(0) & χ'(0) due to numerous λ with N_b = 0.5, Pr = 4.4, Le = 2.8, Sc = 0.6, γ = 1.6, M = 0.8, Pe = 0.4, N_t = 0.2, σ = 0.2.

λ	f''(0)	θ'(0)	ϕ'(0)	χ'(0)
0.1	-0.1578	-0.0565	-0.3363	-0.3184
0.3	-0.4918	-0.1354	-0.4538	-0.4060
0.5	-0.8493	-0.2140	-0.5721	-0.4926
0.7	-1.2292	-0.2749	-0.6987	-0.5820
0.9	-1.6303	-0.3227	-0.8234	-0.6694
1.1	-2.0517	-0.3632	-0.9407	-0.7524

In our problem, we have considered small values of porosity parameter γ in fluid flow. This confirms that there are small voids in the porous region. This is why vorticity in the neighborhood through pores has an impact on the flow. Therefore, the porosity parameter has an effect on all quantities discussed in Table 3. We can find out from Table 3 that with the upsurge in the values of porosity parameter γ, shear stress is increasing but $\theta'(0)$, $\phi'(0)$ as well as $\chi'(0)$ are showing decaying behavior.

When the sheet is stretched along x the direction, it has an effect on flow parameters. It may be noted from Table 4 that a rise in values of the stretching parameter λ causes an upsurge in values of all physical quantities $f''(0)$, $\theta'(0)$, $\phi'(0)$ and $\chi'(0)$.

Figs. (2-5) depict the stimulus of magnetic parameter M on $f'(\eta)$, $\theta(\eta)$, $\chi(\eta)$ and $\phi(\eta)$. It is observed that with the enhancement in both electric conductivity of fluid and strength of the magnetic field, the magnetic parameter boosts. Fig. 2 portrays that with the increase in M, the velocity profiles have decreasing conduct. Figs. 3 & 5 confirm that with the upsurge in M values, the curves of temperature and motile microorganisms' density are rising. It is evident from Fig. 4 that with the rise in M values, nanoparticles' volume fraction profiles are growing.

We have perceived that there are two possibilities for λ, it is either positive or negative. As the sheet is stretched out, the flow velocity upsurges. It may be observed from Figure 6 that the growth of stretching parameter λ tends to enhance velocity distribution. Figure 7 makes us clear that as λ rises, profiles of $\theta(\eta)$ downturn. Similarly, it is shown in Figures 8 & 9 that enhancement in values of stretching factor leads to uplift curves of $\phi(\eta)$ as well as $\chi(\eta)$.

Figs. 10-13 illustrate the impact of porosity parameter γ on the profiles of physical quantities involved in the flow problem. It can be seen from Figure 10 that an upsurge in porosity parameter γ leads to a drop in velocity distribution. Fig. 11 demonstrates that as the values of γ rise, profiles of $\theta(\eta)$ are escalating. One may observe from Fig. 12 that with the enhancement in the values of the porosity parameter the profiles of $\phi(\eta)$ are inclining. Fig. 13 portrays that as γ values grow, the profiles of nanoparticles' volume fraction are inclining.

CONCLUSIONS

We have numerically surveyed MHD nanofluid flow with gyrotactic microorganisms due to a sheet embedded in porous media. We have illustrated impressions of

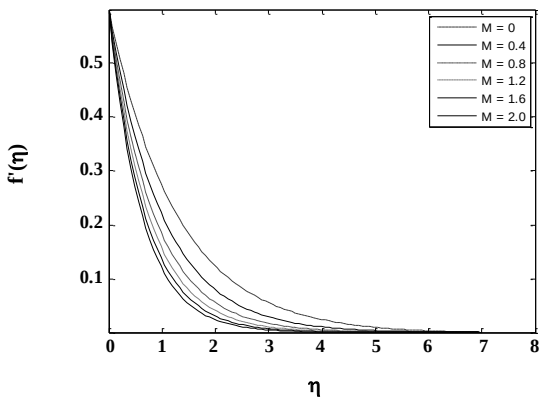

Fig. 2: f'(η) profiles due to numerous M and λ = 0.6, Pr = 4.3, Le = 1.6, Sc = 1.2, γ = 0.02, N_t = 0.7, Pe = 0.2, N_b = 0.3, σ = 0.2.

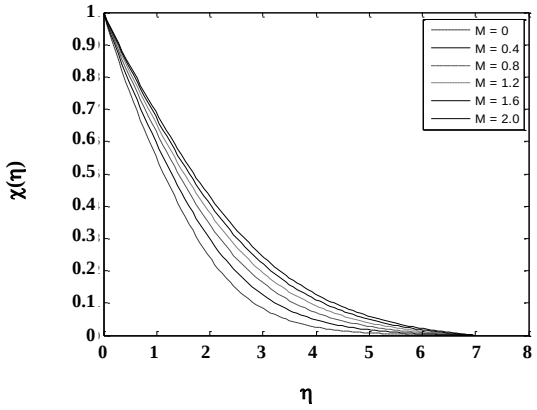

Fig. 5: χ(η) profiles due to numerous M and λ = 0.6, Pr = 4.3, Sc = 1.2, Le = 1.6, γ = 0.02, N_t = 0.7, Pe = 0.2, N_b = 0.3, σ = 0.2.

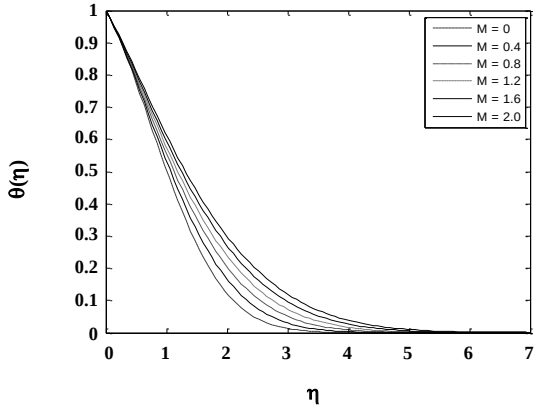

Fig. 3: θ (η) profiles due to numerous M and λ = 0.6, Pr = 4.3, Le = 1.6, Sc = 1.2, γ = 0.02, N_t = 0.7, Pe = 0.2, N_b = 0.3, σ =0.2.

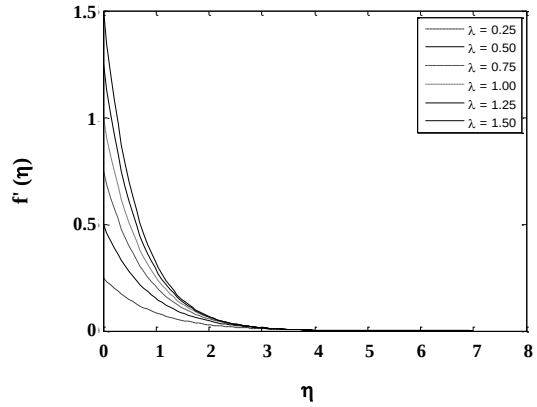

Fig. 6: f'(η) profiles due to numerous λ > 0 and Pr = 1.7, N_b = 0.7, Le = 2.3, N_t = 0.7, M = 0.9, γ = 0.02, Sc = 1.2, Pe = 0.2, σ =0.2.

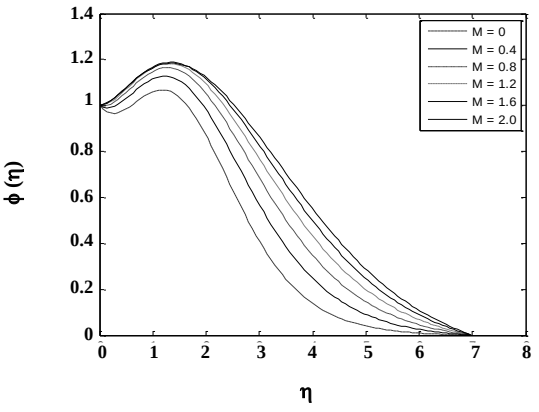

Fig. 4: ϕ(η) profiles due to numerous M and λ = 0.6, Pr = 4.3, Sc = 1.2, Le = 1.6, γ 0.02, N_t = 0.7, Pe = 0.2, N_b = 0.3, σ =0.2.

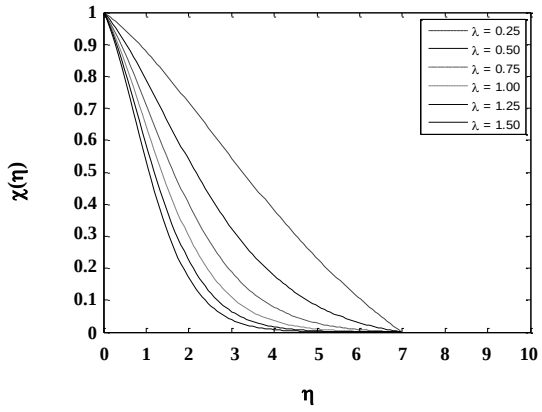

Fig. 7: θ(η) profiles due to numerous λ > 0 and Pr = 1.7, N_b = 0.7, Le = 2.3, N_t = 0.7, M = 0.9, γ = 0.02, Sc = 1.2, Pe = 0.8, σ =0.2.

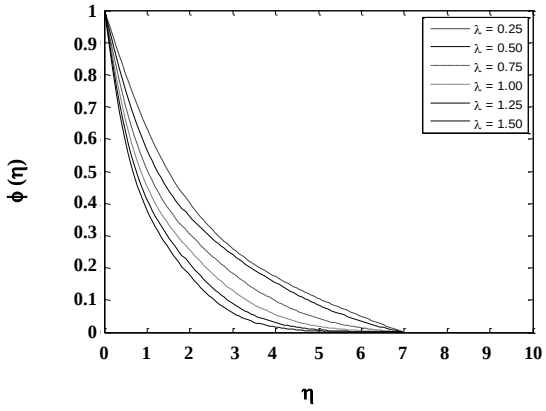

Fig. 8: $\phi(\eta)$ profiles due to numerous $\lambda > 0$ and Pr = 1.7, N_b = 0.7, Le = 2.3, N_t = 0.7, M = 0.9, γ = 0.02, Sc = 1.2, Pe = 0.8, σ=0.2.

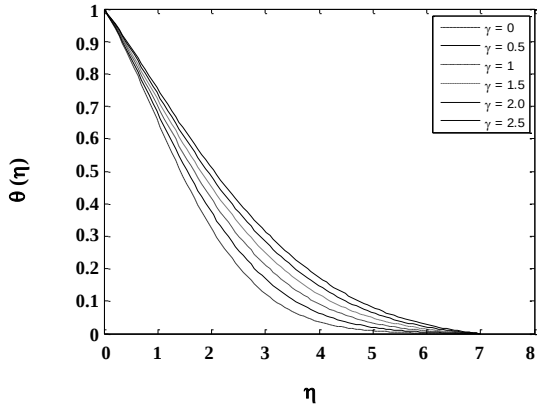

Fig. 11: $\theta(\eta)$ profiles due to numerous γ and N_b = 0.3, Pe = 0.2, λ = 0.5, Le = 2.3, Pr = 3.7, M = 0.9, N_t = 0.7, Sc = 1.2, σ = 0.2.

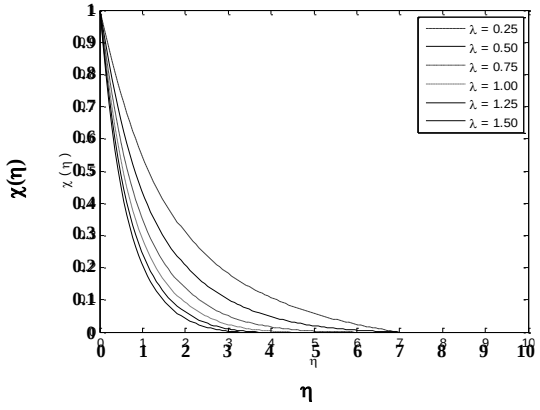

Fig. 9: $\chi(\eta)$ profiles due to numerous $\lambda > 0$ and Pr = 1.7, N_b = 0.7, Le = 2.3, N_t = 0.7, M = 0.9, γ = 0.02, Sc = 1.2, Pe = 0.8, σ=0.2.

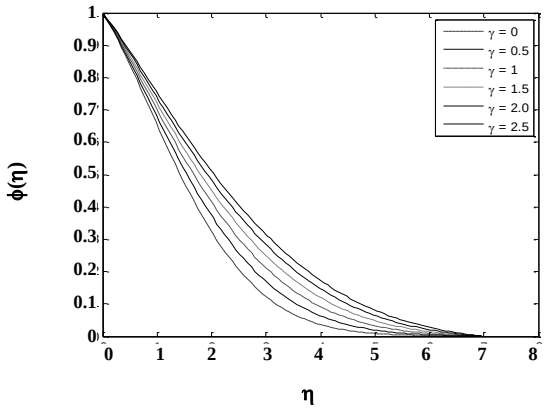

Fig. 12: $\phi(\eta)$ profiles due to numerous γ and N_b = 0.3, Pe = 0.2, λ = 0.5, Le = 2.3, Pr = 3.7, M = 0.9, N_t = 0.7, Sc = 1.2, σ = 0.2.

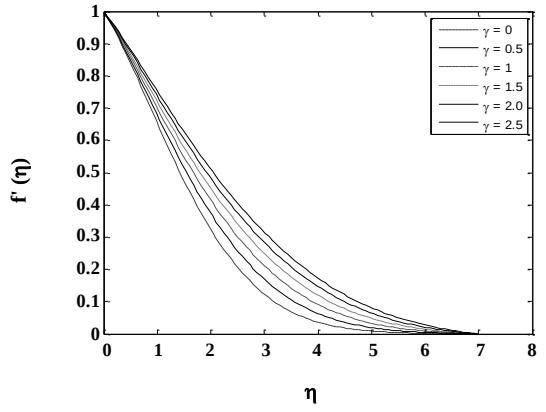

Fig. 10: f'(η) profiles due to numerous γ and N_b = 0.3, Pe = 0.2, λ = 0.5, Le = 2.3, Pr = 3.7, M = 0.9, N_t = 0.7, Sc = 1.2, σ = 0.2.

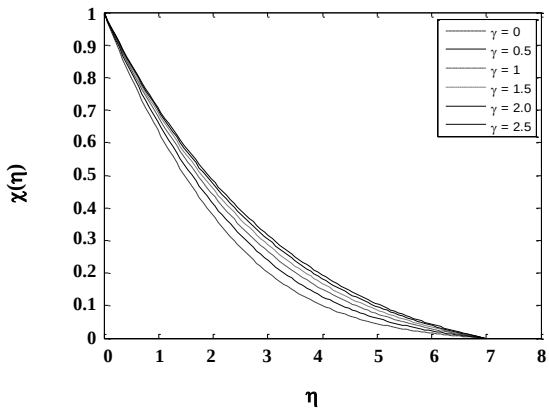

Fig. 13: $\chi(\eta)$ profiles due to numerous γ and N_b = 0.3, Pe = 0.2, λ = 0.5, Le = 2.3, Pr = 3.7, M = 0.9, N_t = 0.7, Sc = 1.2, σ = 0.2.

different parameters on physical measures with the assistance of tables as well as figures. The important discoveries of eminent parameters of our problem are as follows:

- The applied magnetic field tends to rise the shear stress while reducing heat transfer rate, rate of nanoparticles volume fraction, and microorganism's density rate.
- The porosity parameter causes a reduction in velocity distribution while it grows profiles of the other three measures.
- The magnetic parameter demotes the velocity distribution while the stretching parameter boosts the velocity profiles.
- The porosity parameter and stretching parameter $\lambda>0$ enhance the shear stress.
- The magnetic parameter and stretching parameter significantly elevate the temperature distribution, whereas an upsurge in the porosity parameter drops temperature profiles.

Nomenclature

u	Velocity in the x-direction
v	Velocity in the y-direction
μ	Dynamic viscosity
υ	Kinematic viscosity
ρ_{fl}	Fluid's density
ρ_{pr}	Particle's density
T	Temperature
c_p	Specific heat
a_o	Positive constant
D_t	Thermophoresis diffusion coefficient
D_b	Brownian coefficient
D_m	Microorganism diffusion coefficient
σ_{ec}	Electric conductivity
W_{cs}	Maximum swimming speed of cell
K_0	Thermal conductivity
v_{ch}	Chemotaxis constant
α	Thermal diffusivity
B_0	Strength of magnetic field
n	Microorganisms' concentration
c	Volume fraction of nanoparticles
M	Magnetic parameter
Pr	Prandtl number
Le	Lewis number
Sc	Schmidt number
N_b	Brownian motion parameter
N_t	Thermophoresis parameter
Pe	Peclet number
σ	Constant term
λ	Stretching parameter
γ	Porosity parameter
η	Dimensionless variable

Received : Jan. 15, 2020 ; Accepted :Oct. 6,2020

REFERENCES

[1] Mahat R., Noraihan A.R., Shafie S., Kasim A.R.M., Mixed Convection Boundary Layer Flow of Viscoelastic Nanofluid Past a Horizontal Circular Cylinder with Convective Boundary Condition, *Int. J. Mech. Eng. Robot. Res*., **8(1)**: 87-91 (2019).

[2] Hosseinzadeh K., Alizadeh M., Ganji D.D., Hydrothermal Analysis on MHD Squeezing Nanofluid Flow in Parallel Plates by Analytical Method, *Int. J. Mech. Mater. Eng*., **13(4)**: (2018).

[3] Muhammad S., Ishaq M., Hussain A.S., Khan H., Ali G., Shah S.I.A., Radiative Heat Transfer and Magneto Hydrodynamics Bioconvection Model for Unsteady Squeezing Flow of Nanofluid with Sort and Dufour Effects Between Parallel Channels Containing Nanoparticles and Gyrotactic Microorganisms, *J. Nanofluids*, **8(7)**: 1433-1445 (2019).

[4] Aziz R.C., Hashim I., Abbasbandy S., Flow and Heat Transfer in a Nanofluid Thin Film Over an Unsteady Stretching Sheet, *Sains Malaysiana*, **47(7)**:1599-1605 (2018).

[5] Iqbal M.F., Ahmad S., Ali K., Akbar M. Z., Ashraf M., Analysis of Heat and Mass Transfer in Unsteady Nanofluid Flow Between Moving Disks with Chemical Reaction-A Numerical Study, *Heat Transfer Res.*, **49(14)**: 1403-1417 (2018).

[6] Abbas T., Hayat T., Ayub M., Bhatti M. M, Alsaedi A., Electromagnetohydrodynamic Nanofluid Flow Past a Porous Riga Plate Containing Gyrotactic Microorganism, *Neural Computing and Applications*, **31(6)**: 1905-1913 (2019).

[7] Sibanda P., Khidir A., Nanofluid Flow Over a Nonlinear Stretching Sheet in Porous Media with MHD and Viscous Dissipation Effects, *J. of Por. Med.*, **17(5)**: 391-403 (2014).

[8] Aghbari A., Sadaoui D., Agha H. A., Viscous Dissipation Effect for Double Diffusive Free Convection Flow along a Vertical Plate Embedded in a Porous Medium Saturated with a Nanofluid, *ICHMT Digital Library Online*, 693-704(2017).

[9] Kumar M., Mishra A., Viscous Dissipation and Joule Heating Influences Past a Stretching Sheet in a Porous Medium with Thermal Radiation Saturated by Silver-Water and Copper-Water Nanofluids, *Special. Topics. Rev. Por. Med.: Int. J.*, **10(2)**: 171-186 (2019).

[10] Yusuri A. K, Izadi M., Hatami H., Numerical Study of Natural Convection in a Square Enclosure Filled by Nanofluid with a Baffle in the Presence of Magnetic Field, *Iran. J. Chem. Chem. Eng. (IJCCE)*, **38(5)**: 209-220 (2019).

[11] Ashraf M., Ali K. Ashraf M., Numerical Simulation of Micropolar Flow in a Channel Under Oscillatory Pressure Gradient, *Iran. J. Chem. Chem. Eng. (IJCCE)*, **39(2)**: 261-270 (2020).

[12] Gireesha B. J., Krishnamurthy M. R., Prasannakumara B. C., Reddy Gorla R. S., MHD Flow and Nonlinear Radiative Heat Transfer of a Casson Nanofluid Past a Nonlinearly Stretching Sheet in the Presence of Chemical Reaction, *Nanosci. Technol.: Int. J.*, **9(3)**: 207-229 (2018).

[13] Kumar M., Pandey A. K., Effects of Viscous Dissipation and Heat Generation/ Absorption on Nanofluid Flow over an Unsteady Stretching Surface with Thermal Radiation and Thermophoresis, *Nanosci. Technol.: Int. J.*, **9(4)**: 325-341 (2018).

[14] Sampath Kumar P. B., Gireesha B. J., Mahantheth B., Chamkha A. J., Thermal Analysis of Nanofluid Flow Containing Gyrotactic Microorganisms in Bioconvection and Second-Order Slip with Convective Condition, *J. Therm. Anal. Calorim.*, **136(5)**: 1947-1957 (2019).

[15] Sheikholeslami M., Darzi M., Sadoughi M. K., Heat Transfer Improvement and Pressure Drop During Condensation of Refrigerant- Based Nanofluid; An Experimental Procedure, *Int. J. Heat Mass Transfer*, **122**: 643-650 (2018).

[16] Jafaryar M., Sheikholeslami M., Zhixiong Li, Moradi R., Nanofluid Turbulent Flow in a Pipe under the Effect of Twisted Tape with Alternate Axis, *J. Therm. Anal. Calorim*, **135(1)**: 305-323 (2019).

[17] Rashad A. M., Nabwey H. A., Gyrotactic Mixed Bioconvection Flow of a Nanofluid Past a Circular Cylinder with Convective Boundary Condition, *J. Tai. Inst. Chem. Engs.*, **99**: 9-17 (2019).

[18] Ahmad S., Ashraf M., Ali K., Simulation of Thermal Radiation in a Micropolar Fluid Flow through a Porous Medium between Channel Walls, *J. Therm. Anal. Calorim.*, (2020).

[19] Kausar M. S., Hussanam A., Mamat M., Ahmad B., Boundary-Layer Flow through Darcy-Brinkman Porous Medium in the Presence of Slip Effects and Porous Dissipation, *Symmetry*, **11(5)**: (2019).

[20] Vafai K., Tien C. L., Boundary and Inertia Effects on Flow and Heat Transfer in Porous Media, *Int. J. Heat Mass Transfer*, **24(2)**: 195-203 (1981).

[21] Kaviany M., Boundary- Layer Treatment of Forced Convection Heat Transfer from a Semi-Infinite Plate Embedded in a Porous Media, *J. Heat Trans*fer, **109(2)**: 345-349 (1987).

[22] Aman F., Khazim W. M. & Mansur S., Mixed Convection Flow of a Nanofluid Containing Gyrotactic Microoranisms Over a Stretching\Shrinking Sheet in The Presence of Magnetic Field, *J. Phys.:Conf. Ser*, **890**: (2017).